Available online at www.sciencedirect.com
ScienceDirect
Journal of Power Sources 171 (2007) 879–885
JOURNAL OF POWER SOURCES
www.elsevier.com/locate/jpowsour

New freeze-drying method for $LiFePO_4$ synthesis

Verónica Palomares [a], Aintzane Goñi [a], Izaskun Gil de Muro [a], Iratxe de Meatza [b], Miguel Bengoechea [b], Oscar Miguel [b], Teófilo Rojo [a,*]

[a] *Departamento de Química Inorgánica, Universidad del País Vasco UPV/EHU, Apdo. 644, 48080 Bilbao, Spain*
[b] *Departamento de Energía, CIDETEC, P° Miramón 196, Parque Tecnológico de San Sebastián, 20009 San Sebastián, Spain*

Received 8 March 2007; received in revised form 23 May 2007; accepted 24 June 2007
Available online 29 June 2007

Abstract

The freeze-drying method is proposed as an effective synthesis process for the obtaining of $LiFePO_4$/C composites. The citric acid is used as a complexing agent and carbon source. After the low temperature annealing, the freeze-dried solution leads to a homogeneous carbon covered $LiFePO_4$ sample. The chemical characterization of the material included ICP and elemental analysis, infrared spectroscopy, X-ray diffraction, magnetic measurements and thermal analysis. SEM and TEM microscopies indicate an aggregate morphology with tiny particles of lithium iron phosphate inside a carbon matrix. Impedance spectroscopy showed a 8.0×10^{-7} S cm^{-1} conductivity value. Cyclic voltammetry graphics displayed the two peaks corresponding to the Fe(II)/Fe(III) reaction and demonstrated the good reversibility of the material. The specific capacity value obtained at *C*/40 rate was 164 mAh g^{-1}, with a slight decrease on greater *C*-rates reaching 146 mAh g^{-1} at *C*/1. The capacity retention study has evidenced good properties, with retention over 97% of the maximum values in the first 50 cycles, which allows an effective performance of the freeze-dried sample as cathodic material in lithium-ion batteries.

Keywords: $LiFePO_4$; Synthesis; Freeze-drying

1. Introduction

Since the pioneering work of Padhi et al. [1], mixed orthophosphate $LiFePO_4$ has been intensively studied as cathode material for Li-ion batteries [2]. One of the main problems of $LiFePO_4$ is its low electronic conductivity, which limits the electrochemical extraction of lithium and causes a steep fall in charge/discharge capacities at high rates. The control of particle size [3–6], and the presence, in the cathode composite electrode, of highly dispersed conductive substances such as carbonaceous materials [7,8] and some metals [9,10] enhance the charge/discharge performance. These factors (particle size and conductive coating) are largely affected by the method of preparation. Therefore, to produce commercially available $LiFePO_4$ a proper preparative method is an urgent research target.

In the beginning, solid-state reaction was the most common way of synthesizing this cathode material [11–14]. This method implies the addition of a carbon source during or after the process, usually needing an extra grinding or ball-milling step to get a well-made composite [15–18]. The homogeneity of the mixture must be high to avoid the formation of secondary phases, such as Fe_2O_3 or $Li_3Fe_2(PO_4)_3$, that do not contribute to the electrochemical properties of the samples. Commonly, the ceramic process is associated to several calcination steps with fairly high annealing temperatures, which enhances particle growing and favours the sintering of the particles. This makes the Li diffusion paths longer and difficults a good carbon coating on the particles.

Hydrothermal procedure also enhances grain growth, leading to micrometer-sized monocrystals, not covered in carbon [19,20]. However, interesting results have been obtained by adding sucrose [21,22] or carbon multiwall nanotubes [23] during the synthesis, or including a surfactant in the solution to control the particle size [24]. Either coprecipitation – which is also a common synthesis method [25–27] – or emulsion-drying process – that has been tried a few times [28,29] – allows the obtaining of samples with different carbon percentages and particle sizes. Both methods imply an annealing step after the

* Corresponding author. Tel.: +34 946012458; fax: +34 946013500.
E-mail address: teo.rojo@ehu.es (T. Rojo).

0378-7753/$ – see front matter © 2007 Elsevier B.V. All rights reserved.
doi:10.1016/j.jpowsour.2007.06.161

precipitation or precursor-drying process, which has great influence on the particle size [30,31]. In the case of coprecipitation, the particle size is usually above 1 μm, and it has been reported the possible presence of impurities, such as Li_3PO_4.

The main solution route to synthesize $LiFePO_4$ powders is sol–gel method. This procedure is a good choice for various reasons. First, it involves the mixture of the reactants in solution, forming gel complexes, so assures the homogeneity of element distribution. Second, the chelating agent acts as a carbon source, covering the $LiFePO_4$ grains with a conductive layer and preventing grain growth. Third, this method allows the use of mild annealing temperatures, not favouring great particle sizes [32,33]. So, this procedure yields particles on the order of nanometers, always smaller than 1 μm [34–36]. Some other synthesis ways have been used, not so often, to obtain $LiFePO_4$ powders with improved properties, such as spray pyrolysis [37], mechanical alloying (see reference [6]) or microwave processing [38]. Polyol method has recently also been reported as a possible procedure to synthesize nano-sized $LiFePO_4$ [39].

In this paper, we report on a new $LiFePO_4$ synthesis method. The freeze-drying of a citric acid, lithium, iron and phosphate-containing solution favours the creation of lithium iron phosphate small particles and allows the formation of a carbon coating during the synthesis process. The result is a fine powder of $LiFePO_4$/C composite with a good electrochemical performance.

2. Experimental

2.1. Sample preparation

Stoichiometric amounts (10^{-3} mol) of citric acid monohydrate ($C_6H_8O_7{\cdot}H_2O$), ferrous acetate ($FeC_4H_6O_4$), lithium hydroxide hydrate ($LiOH{\cdot}H_2O$) and ammonium dihydrogenophosphate ($NH_4{\cdot}H_2PO_4$) with a molar ratio of 1:1:1:1 were dissolved in 25 ml water. The solution obtained was drop-by-drop frozen under liquid nitrogen and subjected to the freeze-drying process for 48 h in a Telstar Laboratory Freeze-Dryer Cryodos-80. The powder obtained was calcined two times, at 350 and 600 °C, under nitrogen atmosphere. Elemental analysis by ICP-AES (Perkin–Elmer Optima 2000) of the prepared sample agreed well with the stoichiometry of the $LiFePO_4$ compound. A Perkin–Elmer 2400CHN analyzer was employed for determining the carbon amount in the sample, and the result was 16.1%. By this technique, the presence of a 2% of nitrogen was also detected.

2.2. Characterization of the synthesized powder

Infrared transmittance spectrum was recorded using a MATTSON FTIR 1000 spectrometer. Powder diffraction pattern was collected in a Philips PW1710 diffractometer working with Cu Kα radiation at room temperature. Magnetic measurements were carried out in a SQUID magnetometer from 5 K to room temperature under a 0.1 T magnetic field. Thermal analysis was performed with a SDT2960 instrument. The morphological characterization was made by scanning electron microscopy (SEM) using a JEOL JSM-6400 microscope at 20 kV accelerating voltage, and by transmission electron microscopy (TEM) in a Philips CM200 microscope equipped with an EDAX Energy Dispersive X-ray Analysis (EDX).

2.3. Electrochemical measurements

Conductivity measurements were made on disc-shaped pellets at 25 °C with a frequency response analyzer connected to an Autolab PGSTAT30 potentiostat, over a frequency range from 1 MHz to 1 MHz with 100 mV amplitude. The cyclic voltammetry and galvanostatic tests were conducted using Swagelok type cells assembled in an environmentally controlled dry box. The negative electrode was a disk of lithium metal foil. A glass microfibre sheet soaked in a solution of 1 M $LiPF_6$ in EC:DMC (1:1 w/w) was placed between the two electrodes. The composite positive electrode contained 30% of S-black, 9% of binder (polyvinylidene fluoride, PVDF) and 61 wt.% of active material. Cyclic voltammetry (CV) measurements were carried out using a biologic multichannel potentiostat galvanostat (MPG) in the range from 1 V to 4 V versus Li/Li^+ at 0.1 mV s^{-1}, whereas galvanostatic tests were made in an Arbin BT2000 Battery Tester.

3. Results and discussion

3.1. Synthesis and characterization of the sample

The freeze-drying method has been developed, in this work, to prepare $LiFePO_4$/carbon composite cathode materials. This synthesis method has been already proved to be useful to get fine particle size perovskite phases, with application in SOFC fuel cells [40,41]. Several advantages support the choice of this procedure: homogeneous reactants distribution, presence of a carbon source, mild annealing temperatures. The homogeneity of the element distribution in the reaction mixture was provided by using a water-based solution route synthesis. In our case, the citric acid was employed to provide acidic medium in solution, preventing the oxidation of the ferrous ions, and also as a carbon source, affording the network structure of carbon for electronic conduction. The freeze-dried homogeneous precursor needed only moderate conditions of temperature and time to react to form the desired $LiFePO_4$/C composite. The heat treatment in an inert atmosphere favoured the conversion of citric acid into carbon. The content of C in the finally obtained material was 16.1% in weight, so a 25% of the citric acid and acetate conversed into carbon. The elemental analysis also showed a nitrogen percentage of 2%. The presence of nitrogen in the sample can be justified considering the porosity of the carbonaceous material, which can adsorb N_2 from the synthesis atmosphere.

The characterization of the sample showed the existence of a single $LiFePO_4$ crystalline phase. The observed bands in the IR spectrum were all of them assigned to the vibrational modes of the $LiFePO_4$ compound [42,43]. Likewise, all the diffraction peaks from the powder X-ray diffractogram were indexed for the $LiFePO_4$ olivine structure [44], without the appearance of any unknown diffraction maximum. Magnetic susceptibility measurements exhibited the characteristic antiferromagnetic

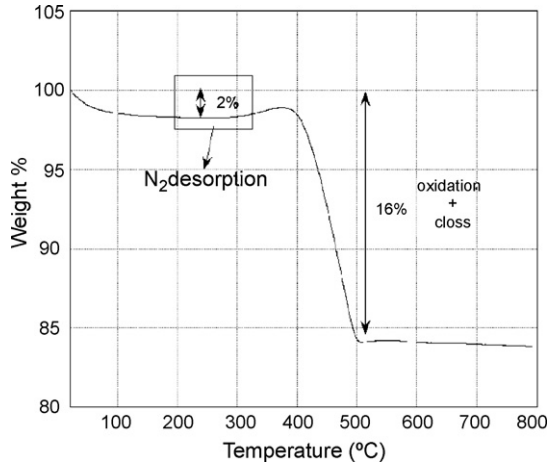

Fig. 1. Thermogravimetric curve of the $LiFePO_4$ sample in air atmosphere.

behaviour of the $LiFePO_4$ material with a Neel temperature of 50 K [45,46]. No anomalies were detected in the thermal evolution of the χ_m values, which indicated the absence of any magnetic additional phase.

Thermogravimetric measurements were carried out by heating the sample at 10 °C min^{-1} in the range from room temperature to 800 °C in air atmosphere. The results are given in Fig. 1. The thermal analysis showed a total mass loss equivalent to 16% of the initial mass. The weight loss takes place in three steps. The first one occurs from room temperature to around 175 °C (mass loss 2%), and it could be attributed to the desorption of approximately 0.05 mol of N_2 per mol of C in the sample. This percentage matches with the elemental analysis results for nitrogen obtained for this sample. The second step takes place from 300 °C up. At this temperature a smooth rise is observed in the thermogravimetric curve, which corresponds to the start of the $LiFePO_4$ oxidation process. This step continues up to 400 °C. At this point the graphic exhibits a steep fall (mass loss 14%), corresponding to the combination of two processes, the oxidation of $LiFePO_4$ started at 300 °C, and the loss of the whole amount of carbon present in the sample. Finally, at 800 °C an intense red residue is obtained. The X-ray diffractogram of this residue confirmed the total absence of $LiFePO_4$ and the coexistence of two Fe(III) compounds, $Li_3Fe_2(PO_4)_3$ and Fe_2O_3. So, the oxidation of the compound during the thermogravimetric study is complete.

The SEM micrographs of the prepared $LiFePO_4$ powder are depicted in Fig. 2. The general appearance of the sample is mostly homogeneous. However, globular grains of sizes smaller than 0.5 μm together with larger aggregates in the range of 1–5 μm are distinguishable. As can be observed in Fig. 2b, the material seems to be framed by an amorphous carbon matrix with the $LiFePO_4$ particles (of sizes smaller than 100 nm) captured inside. The aggregates would be the remainder from the freeze dried metalo-organic network and so, mainly carbon surrounding $LiFePO_4$ particles. Transmission electron microscopy (TEM) and energy dispersive analysis (EDX) were used to confirm this latter point.

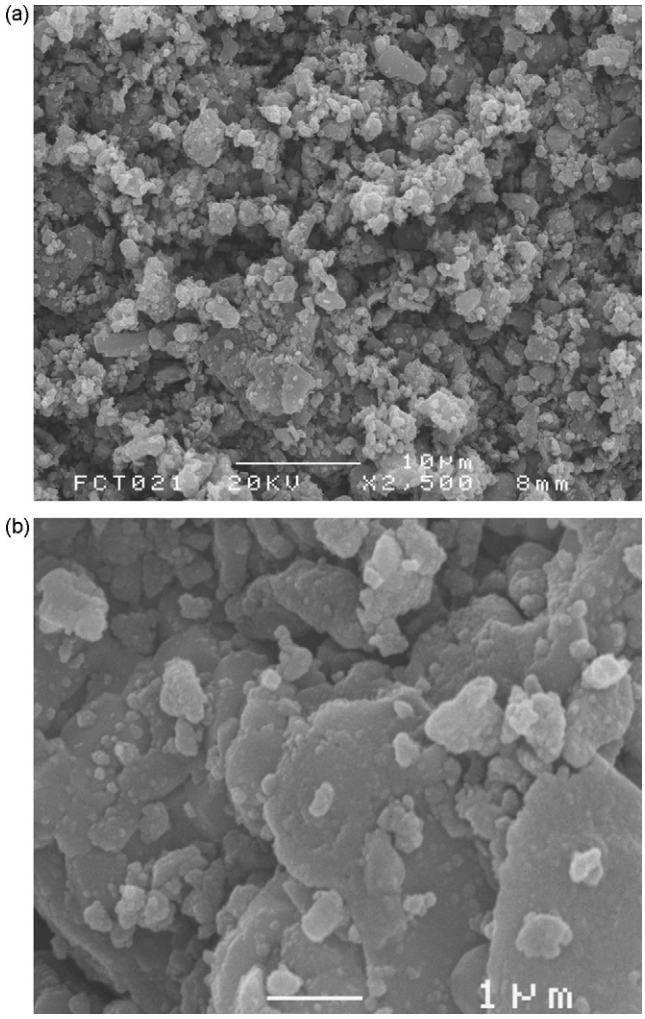

Fig. 2. SEM images from the $LiFePO_4$ sample (a) 2500× and (b) 10,000×.

Fig. 3 shows the TEM images of the sample. As can be seen in Fig. 3a, the nanoparticles of $LiFePO_4$ of about 30 nm size (darker ones) are embedded in a web of lighter nanoparticles identified as carbon by EDX. Diffraction patterns for this C web indicated that it is formed by an amorphous phase, as it was expected for carbon subjected to mild annealing temperatures. Similar particle distribution was observed by Chung et al [47] in their 6 wt.% carbon $LiFePO_4$/C composites. In the case of the freeze-dried sample, the greater amount of carbon, of a 16%, becomes more visible in the micrographs. Moreover, as it can be observed in Fig. 3b, some zones of the composite present an elevated percentage of carbon with few $LiFePO_4$ particles inside. Phosphate particles of greater size, close to 300 nm, are also observed in the material. Those bigger $LiFePO_4$ grains are also surrounded by the same nanocarbon webs (Fig. 3c), although, eventually, they would lose part of their carbon coating during the preparation of the sample for TEM by the ultrasound procedure.

So, the sample exhibits two kinds of carbon coated $LiFePO_4$ particles. A lot of particles are of around 30 nm size, but some of them are larger, of around 300 nm. The last ones appear in the most heterogeneous zones of the material. Therefore, in situ coating of carbon from the pyrolysis of the freeze-drying powder

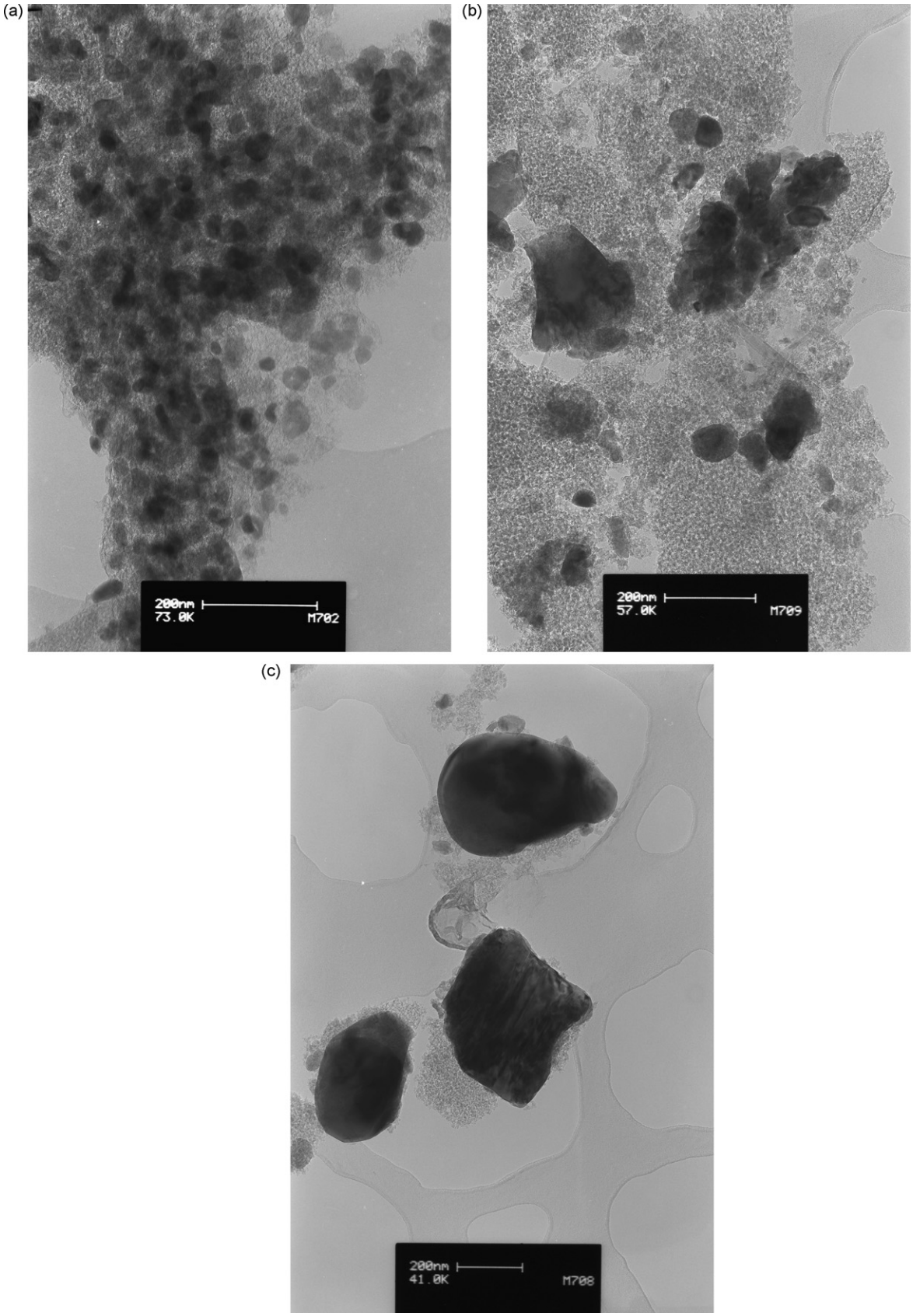

Fig. 3. TEM images of the sample (a) $LiFePO_4$ nanoparticles surrounded by a carbon web; (b) aggregated $LiFePO_4$ particles and amorphous carbon; (c) bigger $LiFePO_4$ grains covered in carbon.

hinders the particle growth efficiently. The nanocarbon webs are effective in preventing the $LiFePO_4$ grain growth, and provide a conducting network that connects all the particles, which must enhance the electrochemical properties of $LiFePO_4$ [48].

3.2. Electrochemical measurements

Impedance spectroscopy measurements showed a conductivity value of 8.0×10^{-7} S cm^{-1}, greater than the theoretical one of 10^{-9} S cm^{-1} (see reference [1]). This increase in the conductivity is due to the presence of carbon in the sample, 16.1% weight. However, higher conductivity values have been reported for materials with lower C percentages (see references [17,32]). The poor conductivity of the carbon present in this freeze-dried $LiFePO_4$/C composite is related to the heat treatment temperature of 600 °C, which was relative low temperature to obtain high conductivity of the carbon.

Fig. 4 shows the cyclic voltammograms of the synthesized $LiFePO_4$/C material. The cathode exhibited sharp oxidation (3.5 V) and reduction (3.3 V) peaks, consistent with a two-phase reaction at about 3.4 V versus Li/Li$^+$. No other peaks are observed, evidencing the absence of electroactive iron impurities. The well-defined peaks, the symmetrical form of the CV plots, and its good reproducibility, confirm the outstanding reversibility of the lithium extraction/insertion reactions in this freeze-dried sample. The discharge curves for cycle 25 are shown in Fig. 5. The cells were cycled between 2 V and 4 V at different current rates. The plateau voltages are almost the same to 3.4 V, and little polarization is observed. The small voltage difference between the charge and discharge plateaus of about 0.2 V at *C*/40, *C*/10, *C*/5 and *C*/1 rates is representative of its good kinetics, especially considering that the electrochemical process involves diffusion of lithium-ions in the solid phase and electrons jumping across a poorly conducting compound. The maximum specific capacity values for the different cycling rates, displayed in Table 1, range from 164 mAh g^{-1} at *C*/40 to 146 mAh g^{-1} at *C*/1. These values are equal to the best-published results for $LiFePO_4$ cathodes (see the references in this article). As it was expected, the specific discharge capacity decreases with increasing *C* rate, due to the low lithium-ion diffusion rate in olivine, but this decrease is slight, only a 4% between *C*/40 and *C*/5, and an 11% at *C*/1. Table 1 also includes the calculated capacity values from the total weight of the $LiFePO_4$/C composite. These values are lower than those calculated versus $LiFePO_4$, since the substantial carbon percentage in the sample, 16%, does not contribute to the specific capacity.

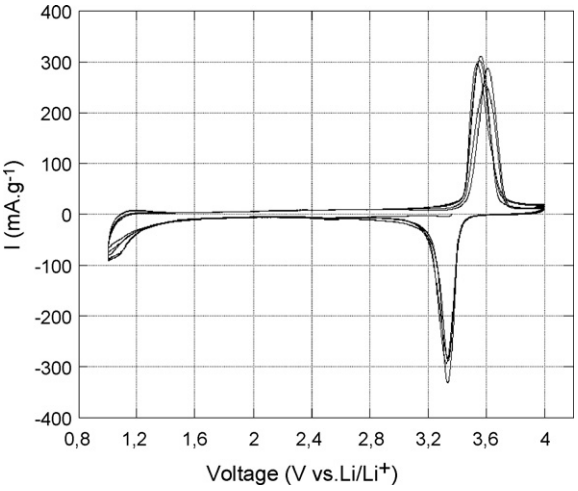

Fig. 4. Cyclic voltammogram of $LiFePO_4$/C at 0.1 mV s^{-1} (four cycles).

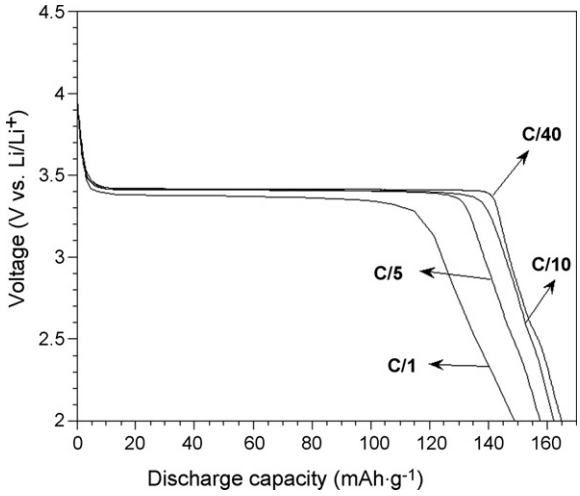

Fig. 5. Discharge curves at different rates at room temperature. First cycle of *C*/40 and 25th cycle of *C*/10, *C*/5 and *C*/1.

Table 1
Specific capacity values for different cycling rates

	Capacity	
	mAh g^{-1}	mAh g^{-1} ($LiFePO_4$/C)$^{-1}$
C/40	164	138
C/10	162	136
C/5	157	132
C/1	146	123
%C	16.1	
σ (S cm^{-1})	8×10^{-7}	

The results of the capacity retention study, at different rates, for the cells prepared with the freeze-dried $LiFePO_4$ composite are shown in Fig. 6. The sample manifests very good cycling performance with a maximum specific capacity of 158 mAh g^{-1} at *C*/10, and smooth capacity fading rate of 0.1 mAh g^{-1} per cycle. The initial gain displayed in the graphic can be due to the great amount of carbon in the sample, that disturbs the penetration of the electrolyte in the cathode. By this phenomenon, the maximum specific capacity of the material is showed after a few cycles (see reference [28]) and it is more pronounced for higher rates as it is expected for a kinetic effect. The good behaviour on cycling has also been observed in the outstanding reversibility of the CV plot. Table 2 shows the capacity retention percent-

Table 2
Capacity retention percentage for 50 cycles at different rates

C/10	97.5
C/5	98
C/1	98.7

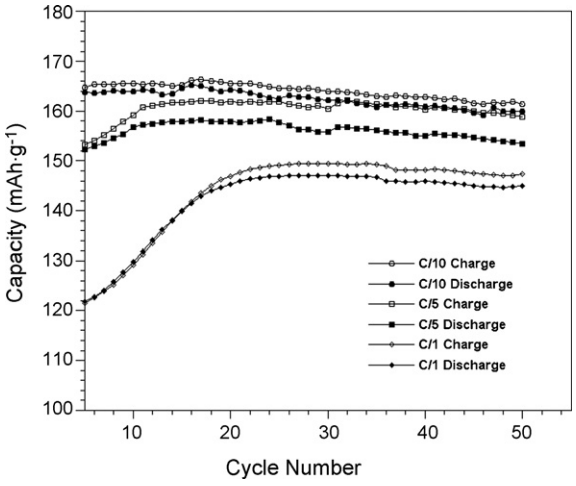

Fig. 6. Capacity retention study at different rates.

age for 50 cycles at different rates. This parameter is, in most cases, over 97% of the maximum specific capacity, in the range showed by other reported samples. This satisfactory response may be attributed to small particle size and a good carbon coating.

A parameter to take into account for practical applications is the "tap density" of the electrode material. The approximate value obtained for $LiFePO_4$/C is $1.2\,g\,cm^{-3}$, a third of $3.6\,g\,cm^{-3}$, the crystallographic density of the compound. The relatively low temperature of firing, in addition to the large fraction of carbon, results in low value of this parameter.

The electrochemical performance of the freeze-dried sample is excellent, in spite of its no perfect homogeneous morphology and its low conductivity value of around $10^{-7}\,S\,cm^{-1}$. Comparing with similar materials obtained by different synthetic methods, this sample offers similar discharge behaviour to those prepared by other solution methods, such as coprecipitation or sol–gel. In order to improve the results, it could be desirable to reduce the amount of carbon in the sample to a medium value of 5%, for example, what would lead to a greater proportion of active material per gram of composite. With this objective, several possibilities are being tried, including the change in complexing agent proportions and the use of oxygen plasma treatment to eliminate part of the carbon produced.

4. Conclusions

The freeze-drying method is a new synthesis procedure useful to prepare $LiFePO_4$/C composites. The obtained material presents the required purity, adequate morphology and a good electrochemical performance. The observed specific capacity values for the different cycling rates are fairly good. The capacity retention study shows very optimistic results, with retention over 97% of the maximum values in the first 50 cycles. Although the sample presents an elevated carbon content of 16.1% weight, its conductivity is slightly lower than observed in other materials with less carbon. This fact indicates that it would be advantageous to reduce the amount of carbon in future samples in order to maximize the active material in the composite.

Acknowledgements

This work was financially supported by the Ministerio de Educación y Ciencia (PTR95.0939.01), the Universidad del País Vasco/Euskal Herriko Unibertsitatea (GIU06-11) and CEGASA GROUP, which we gratefully acknowledge. V.P. thanks UPV/EHU for a grant. We would like also to thank Igor Cantero for his useful help and Amane Lago for her kind experimental assistance with the electrochemical tests.

References

[1] A.K.M. Padhi, K.S. Nanjundaswamy, J.B. Goodenough, J. Electrochem. Soc. 144 (1997) 1188–1194.
[2] M.S. Whittingham, Chem. Rev. 104 (2004) 4271–4301.
[3] M. Takahashi, S. Tobishima, K. Takei, Y. Sakurai, J. Power Sources 97-98 (2001) 508–511.
[4] H. Huang, S.-C. Yin, L.F. Nazar, Electrochem. Solid State Lett. 4 (2001) A170–A172.
[5] A. Yamada, S.C. Chung, K. Hinokuma, J. Electrochem. Soc. 148 (2001) A224–A229.
[6] S. Franger, C. Benoit, C. Bourbon, F. Le Cras, J. Phys. Chem. Solids 67 (2006) 1338–1342.
[7] N. Ravet, J.B. Goodenough, S. Besuer, M. Simoneau, P. Hovington, M. Armand, Proceedings of the Electrochemical Society and the Electrochemical Society of Japan Meeting Abstracts, vol. 99–92, Honolulu Hawaii, October 17–22, 1999 (abstract 127).
[8] N. Ravet, Y. Chouinard, J.F. Magnan, S. Besner, M. Gauthier, M. Armand, J. Power Sources 97/98 (2001) 503–507.
[9] F. Croce, A.D. Epifanio, J. Hassoun, A. Deptula, T. Olczac, B. Scrosati, Electrochem. Solid State Lett. 5 (2002) A47–A50.
[10] K.S. Park, J.T. Son, H.T. Chung, S.J. Kim, C.H. Lee, K.T. Kang, H.G. Kim, Solid State Commun. 129 (2004) 311–314.
[11] A.K. Padhi, K.S. Nanjundaswamy, C. Masquelier, S. Okada, J.B. Goodenough, J. Electrochem. Soc. 144 (1997) 1609–1613.
[12] A.S. Andersson, J.O. Thomas, B. Kalska, L. Haggstrom, Electrochem. Solid State Lett. 3 (2000) 66–68.
[13] A.S. Andersson, B. Kalska, L. Haggstrom, J.O. Thomas, Solid State Ionics 130 (2000) 41–52.
[14] D. Wang, H. Li, Z. Wang, X. Wu, Y. Sun, X. Huang, L. Chen, J. Solid State Chem. 177 (2004) 4582–4587.
[15] X.Z. Liao, Z.F. Ma, Y.S. He, X.M. Zhang, L. Wang, Y. Jiang, J. Electrochem. Soc. 152 (2005) A1969–A1973.
[16] S.S. Zhang, J.L. Allen, K. Xu, T.R. Jow, J. Power Sources 147 (2005) 234–240.
[17] T. Nakamura, Y. Miwa, T. Mitsuharu, Y. Yamada, J. Electrochem. Soc. 153 (2006) A1108–A1114.
[18] C.H. Mi, G.S. Cao, X.B. Zhao, Mater. Lett. 59 (2005) 127–130.
[19] S. Yang, P.Y. Zavalij, M.S. Whittingham, Electrochem. Commun. 3 (2001) 505–508.
[20] S. Tajimi, Y. Ikeda, K. Uematsu, K. Toda, M. Sato, Solid State Ionics 175 (2004) 287–290.
[21] S. Franger, F. Le Cras, C. Bourbon, H. Rouault, Electrochem. Solid State Lett. 5 (2002) A231–A233.
[22] S. Franger, F. Le Cras, C. Bourbon, H. Rouault, J. Power Sources 119–121 (2003) 252–257.
[23] J. Chen, M.S. Whittingham, Electrochem. Commun. 8 (2006) 855–858.
[24] G. Meligrana, C. Gerbaldi, A. Tuel, S. Bodoardo, N. Penazzi, J. Power Sources 160 (2006) 516–522.
[25] G. Arnold, J. Garche, R. Hemmer, S. Ströbele, C. Vogler, M. Wohlfahrt-Mahrens, J. Power Sources 119–121 (2003) 247–251.
[26] K.S. Park, K.T. Kang, S.B. Lee, G.Y. Kim, Y.J. Park, H.G. Kim, Mater. Res. Bull. 39 (2004) 1803–1810.
[27] M.-R. Yang, W.-H. Ke, S.-H. Wu, J. Power Sources 146 (2005) 539–543.
[28] S.-T. Myung, S. Komaba, N. Hirosaki, H. Yashiro, N. Kumagai, Electrochim. Acta 49 (2004) 4213–4222.

[29] T.-H. Cho, H.-T. Chung, J. Power Sources 133 (2004) 272–276.
[30] B.Q. Zhu, X.H. Li, Z.X. Wang, H.J. Guo, Mater. Chem. Phys. 98 (2006) 373–376.
[31] C.H. Mi, X.G. Zhang, X.B. Zhao, H.L. Li, J. Alloy Compd. 424 (2006) 327–333.
[32] K.-F. Hsu, S.-Y. Tsay, B.-J. Hwang, J. Mater. Chem. 14 (2004) 2690–2695.
[33] R. Dominko, M. Bele, M. Gaberscek, M. Remskar, D. Hanzel, J.M. Goupil, S. Pejovnik, J. Jamnik, J. Power Sources 153 (2006) 274–280.
[34] M. Piana, B.L. Cushing, J.B. Goodenough, N. Penazzi, Solid State Ionics 175 (2004) 233–237.
[35] M. Gaberscek, R. Dominko, M. Bele, M. Remskar, D. Hanzel, J. Jamnik, Solid State Ionics 176 (2005) 1801–1805.
[36] J. Yang, J.J. Xu, J. Electrochem. Soc. 153 (2006) A716–A723.
[37] G.X. Wang, S.L. Bewlay, K. Konstantinov, H.K. Liu, S.X. Dou, J.-H. Ahn, Electrochim. Acta 50 (2004) 443–447.
[38] M. Higuchi, K. Katayama, Y. Azuma, M. Yakawa, M. Suhara, J. Power Sources 119–121 (2003) 258–261.
[39] D.-H. Kim, J. Kim, Electrochem. Solid State 9 (2006) A439–A442.
[40] L. Ortega San Martín, J.P. Chapman, E. Hernández Bocanegra, M. Insausti, M.I. Arriortua, T. Rojo, J. Phys. Condens. Mater. 16 (2004) 3879–3888.
[41] L. Ortega San Martín, J.P. Chapman, J. Sánchez Marcos, J. Rodríguez Fernández, M.I. Arriortua, T. Rojo, J. Mater. Chem. 15 (2005) 183–193.
[42] A.A. Salah, P. Jozwiak, J. Garbarczyk, K. Benkhouja, K. Zaghib, F. Gendron, C.M. Julien, J. Power Sources 140 (2005) 370–375.
[43] C.M. Burba, R. Frech, J. Electrochem. Soc. 151 (2004) A1032–A1038.
[44] D. Destenay, Mem. Soc. Roy. Sci. Liege 10 (1950) 5–28.
[45] R.P. Santoro, R.E. Newham, Acta Crystallogr. 22 (1967) 344–347.
[46] D. Arčon, A. Zorko, R. Dominko, Z. Jagličič, J. Phys. Condens. Mater. 16 (2004) 5531–5548.
[47] H.-T. Chung, S.-K. Jang, H.W. Ryu, K.-B. Shim, Solid State Commun. 131 (2004) 549–554.
[48] H.C. Shin, W.I. Cho, H. Jang, Electrochim. Acta 52 (2006) 1472–1476.